Brake Failure from Residual Magnetism in the Mars Exploration Rover Lander Petal Actuator

Louise Jandura*

Abstract

In January 2004, two Mars Exploration Rover spacecraft arrived at Mars. Each safely delivered an identical rover to the Martian surface in a tetrahedral lander encased in airbags. Upon landing, the airbags deflated and three Lander Petal Actuators opened the three deployable Lander side petals enabling the rover to exit the Lander. Approximately nine weeks prior to the scheduled launch of the first spacecraft, one of these mission-critical Lander Petal Actuators exhibited a brake stuck-open failure during its final flight stow at Kennedy Space Center. Residual magnetism was the definitive conclusion from the failure investigation. Although residual magnetism was recognized as an issue in the design, the lack of an appropriately specified lower bound on brake drop-out voltage inhibited the discovery of this problem earlier in the program. In addition, the brakes had more unit-to-unit variation in drop-out voltage than expected, likely due to a larger than expected variation in the magnetic properties of the 15-5 PH stainless steel brake plates. Failure analysis and subsequent rework of two other Lander Petal Actuators with marginal brakes was completed in three weeks, causing no impact to the launch date.

Introduction

Two Mars Exploration Rover (MER) spacecraft were sent to Mars, each with a rover to explore the Martian surface with its suite of instruments. After entering the Martian atmosphere in an aeroshell, the rovers were delivered to the surface in a Lander covered in airbags. Once the landing system came to rest on the Martian surface and the airbags deflated, three Lander Petal Actuators (LPAs) opened the three deployable Lander side petals, enabling the rover to exit the Lander. Approximately nine weeks prior to the scheduled launch of the first spacecraft, one LPA exhibited a brake failure during its final flight stow at Kennedy Space Center. The failure analysis of this mission critical actuator and the subsequent rework of two other marginal flight LPAs were all done without causing the launch date to slip.

The MER spacecraft, carrying the rovers called Spirit and Opportunity, were launched on June 10, 2003 and July 7, 2003. These spacecraft successfully landed on Mars on January 3, 2004 and January 24, 2004 respectively. All six LPAs operated without any problems.

Figures 1 and 2 show the LPAs installed in the Lander in both the stowed and deployed configurations. The tetrahedral Lander shape with its three LPA-deployed side petals is inherited from the 1997 Mars Pathfinder (MPF) program [1]. With this arrangement, the Lander can right itself from any side petal onto its base petal by opening that side petal until the Lander center of gravity tips the entire system onto the base petal. The LPA torque requirements for MER were much higher due primarily to the larger mass of the landed system, making a re-flight of the MPF LPA design impossible. The same MPF volume constraints for the LPA were applied to MER so the Lander would fit inside the aeroshell. Maintaining the same volume and nearly the same mass as MPF while producing three times the output torque was a significant challenge for the MER LPA. Each LPA had to develop sufficient torque to lift, overturn and right the Lander should it come to rest on a side petal rather than the base petal. Both the first MER lander and the MPF lander stopped on the base petal. However, the second MER lander came to rest on a side petal, causing that side petal LPA to right the lander. In addition, each LPA had to be able to over-deploy its petal to assist in leveling the Lander for a safe rover egress should it come to rest on uneven terrain. Thus, the actuator's unpowered holding torque (or backdrive torque) had to exceed the reaction load from the weight of the Lander supported on a petal with that petal in the fully deployed position. Petal adjustments were made on each MER lander to aid the rover egress. During petal opening, LPA position

* Jet Propulsion Laboratory, California Institute of Technology, Pasadena, CA

knowledge is provided by an incremental encoder signal constructed in the LPA electronics from the motor commutation sensor signals. The LPA electronics are brushless motor drive electronics, physically

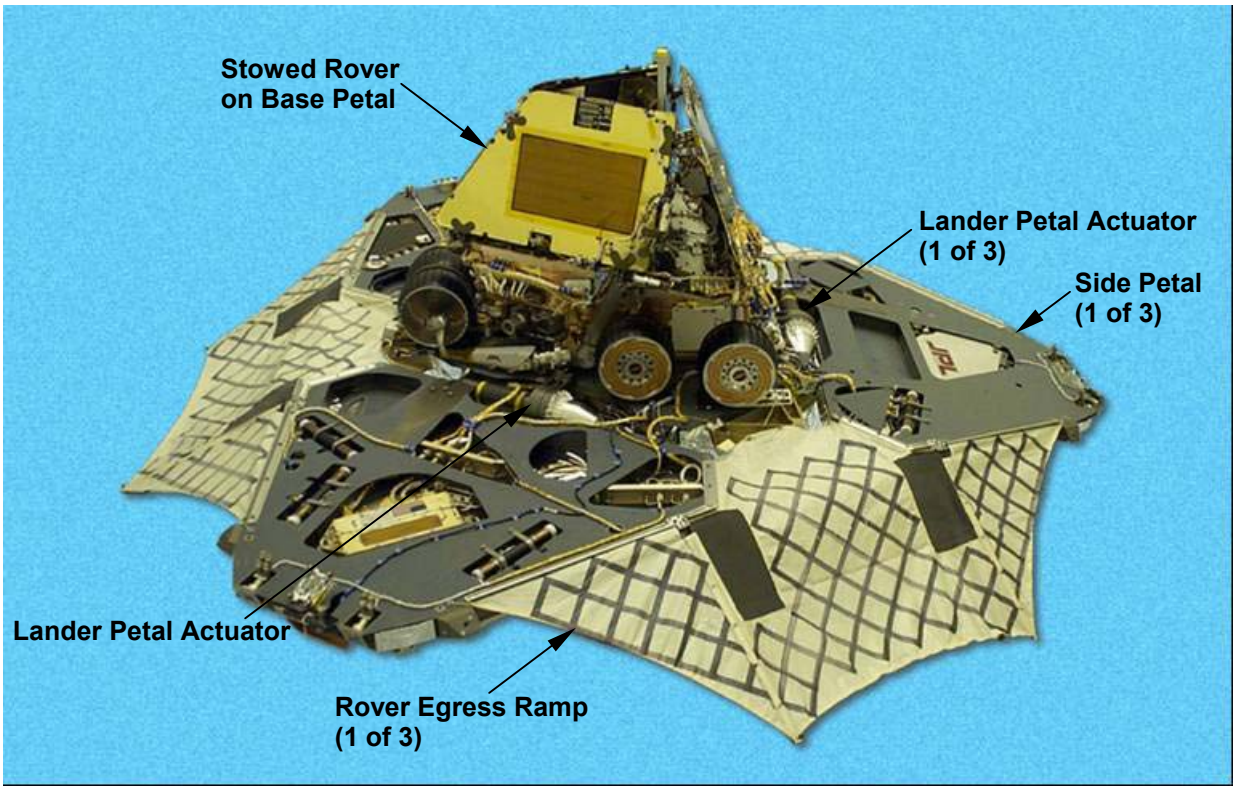

Figure 1. Lander Petal Actuators open each MER Lander side petal to the iron cross position, where all petals are coplanar. Petal motion past this condition is called over-deployed.

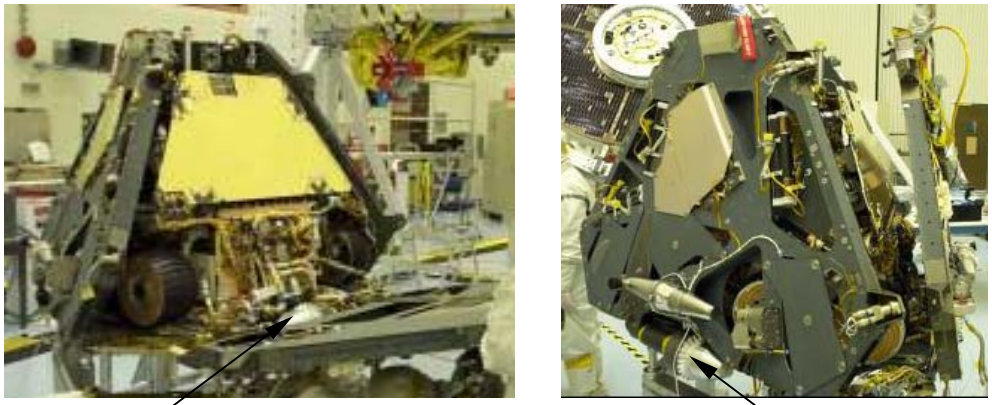

Figure 2. The MER Lander with two side petals stowed and the third side petal closing under the action of its Lander Petal Actuator

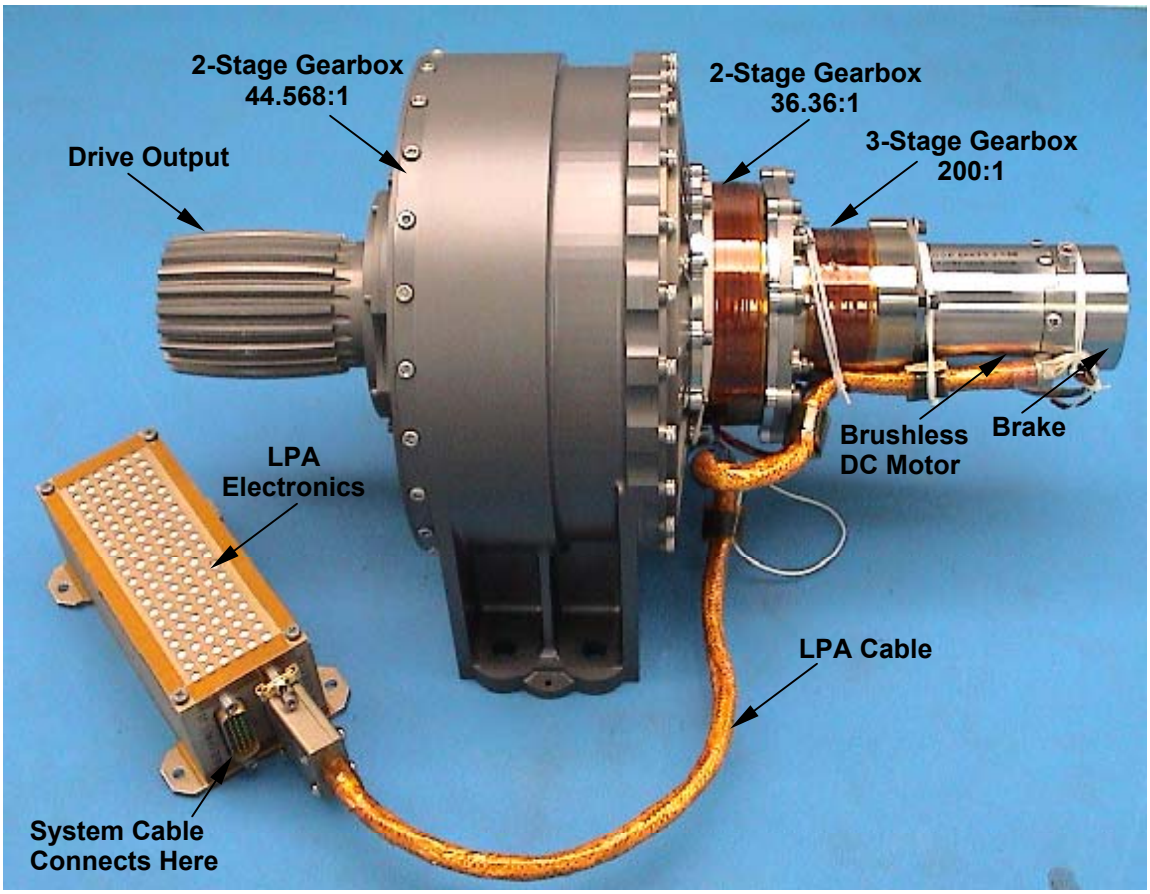

Figure 3. MER Lander Petal Actuator with its electronics

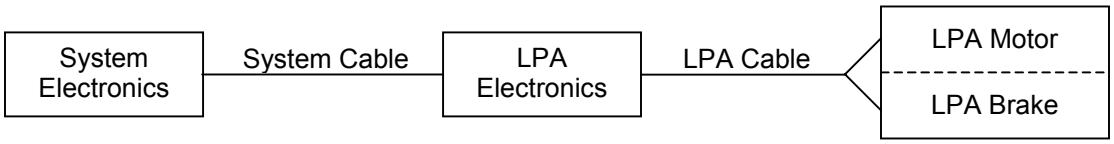

Figure 4. The LPA motor and brake are separately powered and commanded by the system electronics through the LPA electronics, a brushless motor drive electronics.

separate from the LPA and connected by a cable (Figure 3). Potentiometers at each of the petal hinge lines provide additional coarse petal position information, an absolute reference for rover egress.

Lander Petal Actuator

The MER Lander Petal Actuator (Figure 3) is a high torque actuator (3300 N•m output torque) produced by Aeroflex Laboratories, Inc., which consists of a brushless DC motor, a power-off brake, 7 stages of planetary gearing with an overall ratio of 324,099:1, and a crowned spline on the output shaft. The LPA required a brake to meet its backdrive torque requirements with power removed because of the high efficiency of the planetary gearing. The brake is mechanically engaged when non-powered to lock the motor rotor and ensure that the Lander petals cannot move due to external loads. The LPA motor and LPA brake are separately powered and commanded by the system electronics through the LPA electronics (Figure 4). During operation, power is first applied to the LPA brake to release it, followed by

power to the LPA motor to initiate petal motion. At the conclusion of motion, power is first removed from the LPA motor and then the LPA brake to avoid clamping the brake rotor at high speed. All LPAs were tested over temperature at the actuator level to restrain 3300 N•m externally applied to the output shaft. The brake design is a standard spring-applied, power-to-release configuration as shown in the motor/brake assembly cross-section (Figure 5). The brake rotor is attached to the motor rotor. With the brake unpowered, 6 compression springs push the friction plate against the brake rotor, preventing motor rotation. When the brake is energized to release the motor, the friction plate is guided on 3 pins and pulled against the springs by the solenoid. The total stroke of the friction plate is 0.13 mm. There is a 0.051 mm annular non-magnetic shim between the friction plate and the solenoid to break the magnetic flux path and prevent residual magnetism from permanently retaining the friction plate on the solenoid (the stuck-open position).

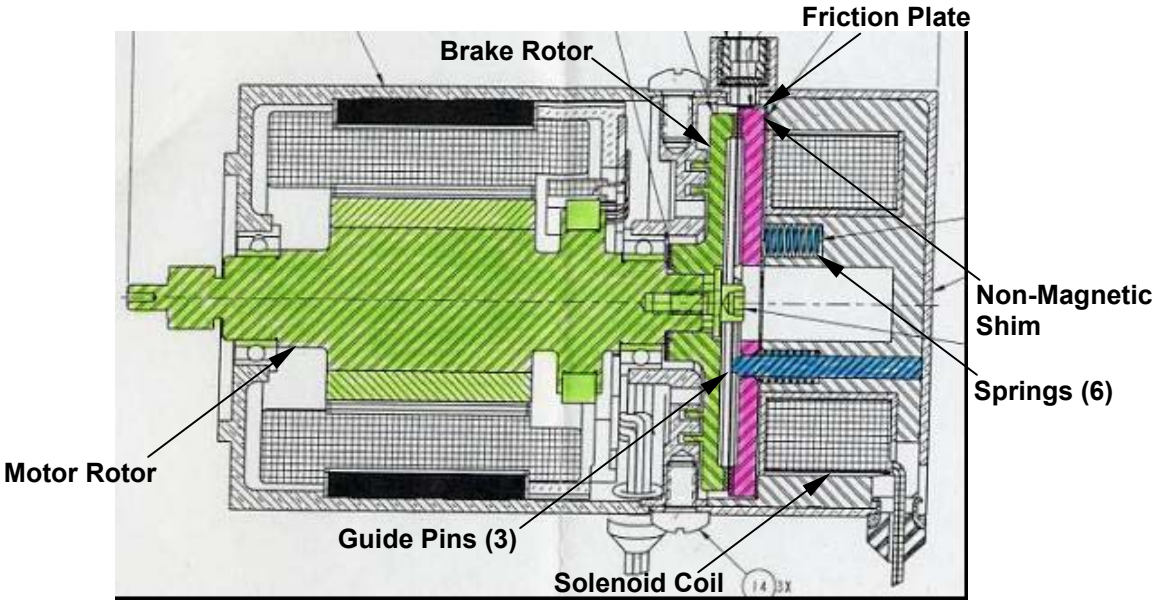

Figure 5. Cross-section of the Lander Petal Actuator motor/brake assembly

Failure and Failure Investigation

The LPA failure occurred about nine weeks before the scheduled launch of the first MER spacecraft. In preparation for closing the Lander for the last time, the spacecraft commanded the Lander petals through their range of motion using the LPAs so that cabling and other hardware near the hinge line could be observed for proper installation and clearance. Although the petals had been moved with the LPAs many times before, this was the first time that all the hardware including the flight airbags was installed during the motion. During a pause in the final flight stow sequence of the Lander petals using the LPAs, one petal drifted downward under gravity with the spacecraft unpowered. The weight of the assembled petal applied about 418 N•m of torque to the LPA output shaft or 13% of the tested backdrive resistance. A load of this magnitude clearly should not have caused the actuator to backdrive with the brake engaged. The failure was initially observed visually as an offset between the commanded position and the actual position. One petal seemed lower than it should be. A check of spacecraft telemetry from the hinge line potentiometers indicated that there was continued motion after completion of the commanded motion, on one petal only, although the current draw from the brake was as expected during the motion and went to zero upon completion of the motion. Once a problem was suspected, the continued motion was also visually observed. The anomaly was repeatable. In a separate check, the suspect petal moved when the LPA was commanded without energizing the brake, a further sign that the brake was not performing properly.

Even though all evidence pointed toward a problem with the LPA brake, a brake failure did not seem credible. Swift, decisive action was required to prevent a launch delay, however the closeness to launch made it even more critical to conclusively isolate the problem prior to removing the hardware from the spacecraft. Uncertainty in determining the cause of the problem would jeopardize the launch. The problem was conclusively isolated to the actuator using the following rationale. With the petal backdriving, the spacecraft was powered off and the connectors between the spacecraft, the LPA drive electronics, and the LPA were demated sequentially until the LPA was completely isolated from the rest of the system. The petal was still backdriving, which conclusively placed the failure in the actuator, eliminating the possibility that a stray current in the system or the drive electronics was keeping the brake powered and in the open position. The failed LPA (SN 007) was removed from the Lander and replaced by a flight spare and failure analysis began on the removed LPA. The failure investigation was conducted at Kennedy Space Center to eliminate the possibility that the failure would be lost during transportation of the LPA to either the Jet Propulsion Laboratory or Aeroflex Laboratories, Inc.

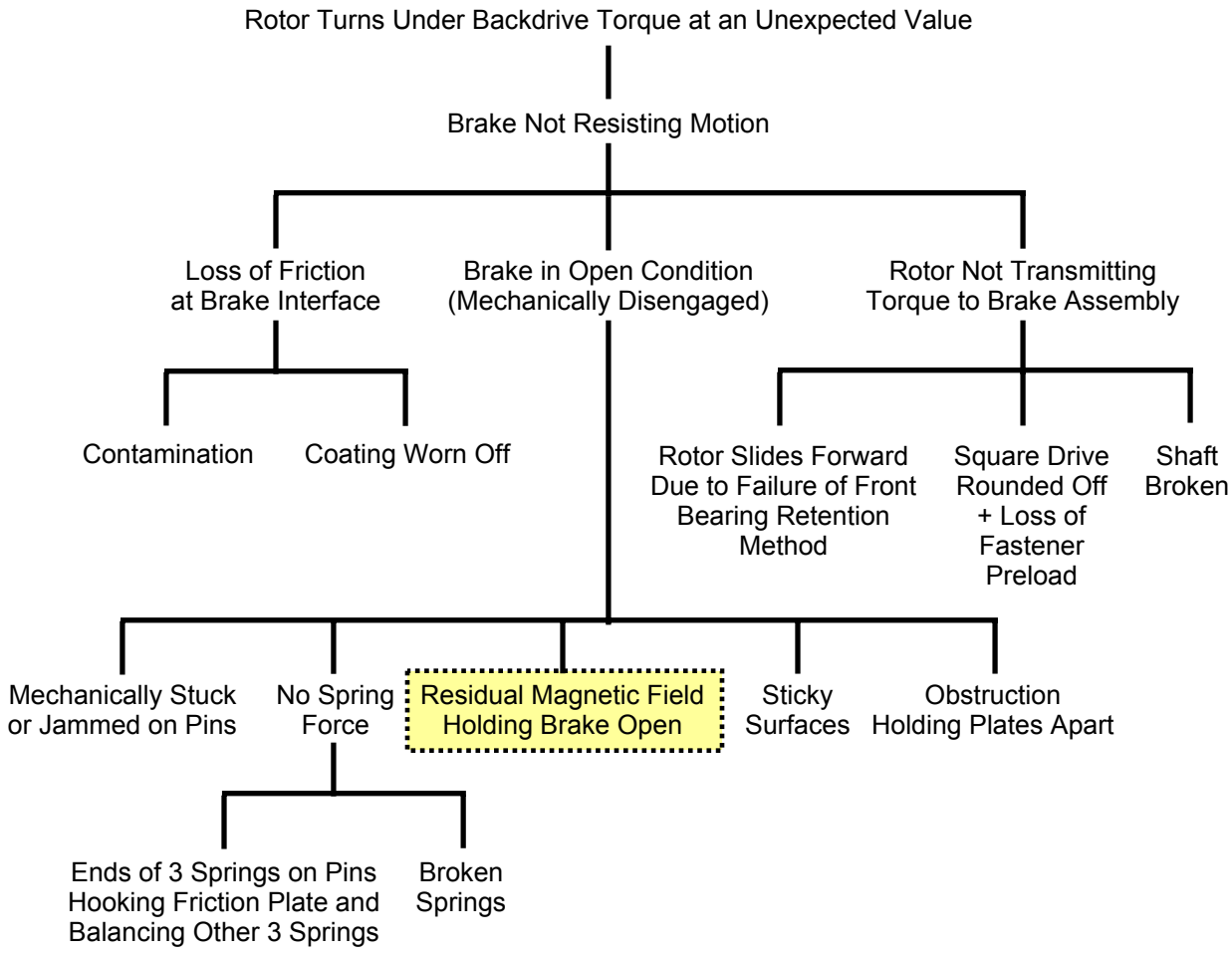

Figure 6. Fault tree for LPA brake failure with the actual failure highlighted in the dotted box

The evidence at this point only indicated that the brake was not resisting motion. Many different failure possibilities were considered which fell into the following general categories: “Brake in Open Condition”; “Loss of Friction at Brake Interface”; or “Rotor Not Transmitting Torque to Brake Assembly” (Figure 6). Many of the failures could only be observed through disassembly of the brake and some of these had the additional unfortunate characteristic that disassembly could cause the loss of the failure. After visual examination of the LPA indicated nothing unusual, the motor was operated with no power to the brake. Motor current indicated no-load operation, which meant the failure was still intact. Real time X-ray examination revealed the brake in a fully disengaged position even though no power was applied to the

brake. This observation eliminated two of the three branches of the fault tree, leaving only the failures listed under “Brake in Open Condition”. No tilting of the friction plate was apparent and nothing unusual was observed in the brake assembly. The only failure remaining that could be determined without disassembly was “Residual Magnetic Field Holding Brake Open”. While still under X-ray examination, a reverse polarity voltage was slowly applied to the brake starting at 0 volts, a demagnetizing action for the friction plate. At negative 0.3 volts, the friction plate moved to the engaged position against the motor rotor indicating the failure was caused by residual magnetism holding the friction plate against the solenoid even though a non-magnetic washer was in the assembly to prevent this particular failure. The motor stalled when operated again with the brake unpowered proving that the demagnetized brake was now fully mechanically engaged. Residual magnetism was the source of the failure in this LPA!

Assessment of Other LPAs

A survey of the acceptance test data for all LPA brake assemblies was performed as a consequence of the SN 007 LPA brake failure. Particular attention was given to the pull-in and drop-out voltages for the brake assemblies since these measurements are an indication of the electromechanical performance of the units. With no voltage applied to the brake, the friction plate is pressed against the brake rotor by the compression springs. Pull-in voltage is measured by slowly raising the brake voltage from zero volts until the friction plate is pulled in to the solenoid, mechanically disengaging from the brake rotor and permitting the motor to turn when the motor is powered with its drive electronics. Figure 7 illustrates the force balance for pull-in. Increasing the voltage across the brake coil causes the current in the solenoid to increase. As the current increases, the magnitude of the magnetic field increases thereby increasing the magnetic force, F_M, on the friction plate. The two forces that act in opposition to F_M are F_S, the total force from the 6 compression springs, and F_f, the friction force between the 3 guide pins and the friction plate. When the magnetic force exceeds the sum of the spring and friction forces, or

$$F_M > F_S + F_f \tag{1}$$

the friction plate moves away from the brake rotor and toward the solenoid, mechanically disengaging the brake. Once motion starts, the brake plate moves quickly open since F_M increases much faster than F_S as the air gap decreases. F_M is a squared function of air gap while F_S is a linear function.

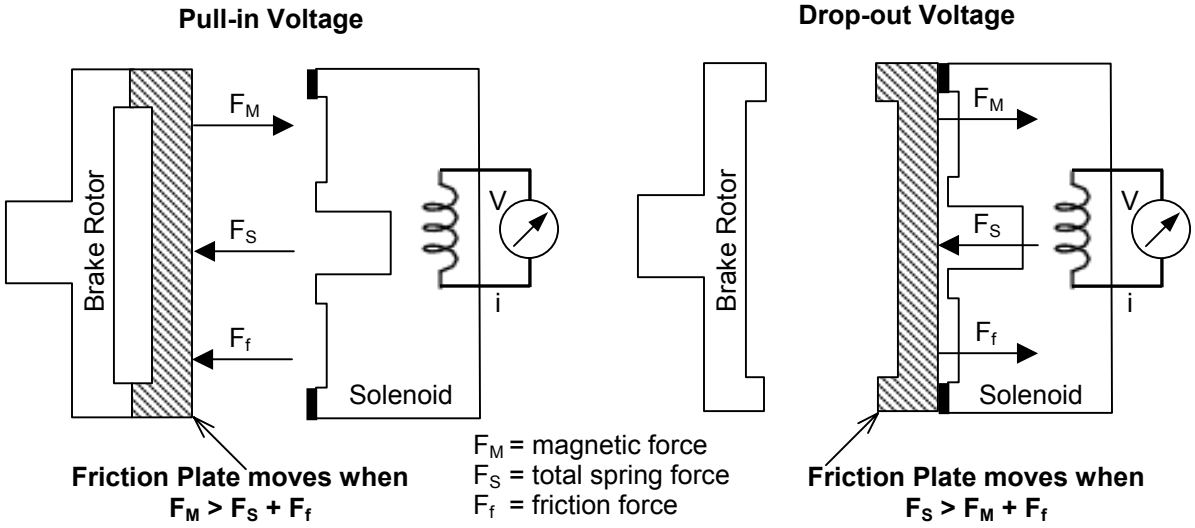

Figure 7. Force balance for brake pull-in and drop-out voltages

Drop-out voltage is then measured by slowly lowering the voltage until the friction plate releases from the solenoid, mechanically engaging the brake rotor again. Figure 7 illustrates the force balance for drop-out. Decreasing the voltage across the solenoid reduces its current and therefore the magnitude of the

magnetic field. As a result, F_M decreases. When the total spring force is sufficient to overcome both the magnetic force and the friction force, or

$$F_S > F_M + F_f \tag{2}$$

the friction plate moves away from the solenoid and reengages the brake rotor. Once motion begins, the friction plate moves quickly to the engaged position since F_M decreases much faster than F_S as the air gap increases. In the case of the failed brake, the condition in equation 2 was not met even though the solenoid voltage and therefore current was zero. F_M was non-zero due to residual magnetism.

The pull-in and drop-out motions of the brake are critical to the operation of the LPA and must be assessed for force margin like any other critical deployment. The desire was to have a force capability of at least twice the force needed to move the components over all conditions of environment and operating voltage. This equates to a minimum factor of safety (the ratio of force capability to force required) of 2.0. The flight brakes were measured to have a pull-in voltage <17 VDC, demonstrating operating margin from the minimum flight input voltage of 24 VDC. The magnetic force is 20 N at 17 VDC and 37.6 N at 24 VDC compared to a maximum total spring force of 10.45 N and an analytically determined maximum friction force of 0.013 N, surpassing the minimum desired force factor of safety for the pull-in deployment by a large amount. Drop-out voltage was measured to be <10 VDC, ensuring adequate separation between the pull-in and drop-out behavior. However no lower threshold on drop-out voltage was defined to ensure operating margin above zero input voltage. The lack of an appropriately specified lower bound for this parameter was an oversight that hindered the discovery of brakes with insufficient force margin for drop-out during acceptance testing. The minimum required force factor of safety for the drop-out deployment was not proven during acceptance testing. Since the failed LPA clearly did not have sufficient margin for drop-out, the other flight LPAs, which were already installed on the flight Landers, were evaluated. The pull-in and drop-out voltages of all LPA brakes were recorded during acceptance testing and measured again after the failure (Table 1). Although the failed unit had the lowest measured value of drop-out voltage, SN 003 and 008 also had very low values for drop-out voltage, raising suspicions that these two actuators might also have insufficient margin for drop-out. A proper specification of drop-out voltage defining sufficient force margin was needed to properly evaluate the flight LPAs and determine if rework was required. LPAs were switched between the two landers, placing the three flight LPAs with the highest values of drop-out voltage on the first lander being prepared for launch. This allowed preparations to continue on the most time-critical lander while the LPA assessment continued, maximizing the chance that the failure could be addressed without impacting either launch.

Table 1. LPA Pull-In and Drop-Out Voltage Measurements

SN [(a)]Failed Unit	Acceptance Test Values (VDC)		As Remeasured (VDC)		Type of Unit
	Pull-In	Drop-Out	Pull-In	Drop-Out	
001	14.1	2.2	12.3	2.22	Qualification
002	Not avail.	Not avail.	12.9	3.25	Flight
003	14.3	1.9	13.6	0.79	Flight
004	12.0	5.0	15.9	3.79	Flight
005	15.5	1.0	Not meas.	Not meas.	Testbed
006	14.07	2.6	14.1	2.40	Flight
007[(a)]	12.7	0.6	12.8	-0.3, 0.29	Flight
008	13.7	1.1	11.7	1.25	Flight
009	12.8	1.72	12.2	1.02	Testbed
010	15.1	0.85	Not meas.	Not meas.	Testbed
011	13.8	2.3	13.7	2.54	Flight Spare

There is no way to take a direct measurement of force in the brake assembly on the fully assembled LPA, therefore there is no way to directly verify the force margin for drop-out on each LPA. Since drop-out voltage is the only easily acquired measurement on the fully assembled LPA, what was needed was a relationship between drop-out voltage and force so that a minimum force factor of safety of 2.0 could be guaranteed. A series of tests was performed on a spare brake assembly to determine how drop-out

voltage varied with spring force. The nominal spring force was calculated from the spring constant and the geometry of the brake assembly. Starting with the friction plate pulled in against the solenoid, the voltage to the brake was lowered until the plate moved under the force of the springs. Reducing the number of springs in the brake assembly decreased the spring force pushing on the friction plate until the brake plate no longer dropped out at zero voltage (Table 2). At this condition, the residual magnetic force is greater than the spring force attempting to push the brake plate off the solenoid. An additional test was performed with no springs in the brake assembly. The voltage to the brake was reduced to zero and a measurement of the force required to separate the friction plate from the solenoid was recorded (Table 3). The same measurements were taken after adding a second non-magnetic 0.051 mm shim between the solenoid and the friction plate (Tables 2 and 3). Adding the second shim raised the drop-out voltage significantly (Figure 8) without changing the pull-in voltage substantially. These tests enabled a method to determine the force margin and illustrated a rework path that could increase that margin.

Table 2. Drop-out voltage vs. spring force as measured on a spare brake

# of Springs	0.051-mm shim		2x 0.051-mm shim	
	Nominal Force (N)	Voltage (V)	Nominal Force (N)	Voltage (V)
6	9.012	1.27	8.910	3.60
5	7.508	0.92	7.428	3.21
4	6.005	0.22	5.943	2.12
3	4.506	No release[(b)]	4.457	1.51
2			2.971	0.35
1			1.486	No release

[(b)]No release at zero volts, released with –0.3 volts (reverse polarity voltage of 0.3 volts)

Table 3. Force required to separate the friction plate from the solenoid at zero volts as measured on a spare brake

# of Springs	0.051-mm shim		2x 0.051-mm shim	
	Nominal Force (N)	Voltage (V)	Nominal Force (N)	Voltage (V)
0	4.706	0	2.224	0

The required margin point for each shim condition was determined using the spring force test data and a tolerance analysis of spring force. A quadratic equation was fit to the test data in Figure 8 since force in the solenoid is a quadratic function of current and therefore voltage. Regression results in equations of the form:

$$F_M = aV^2 + bV + c \tag{3}$$

with a, b, and c all constants. Setting c equal to the minimum possible spring force of three springs minus the maximum possible friction force from the alignment pins shifted the curves. This ensures that when six springs are present, there is a minimum factor of safety of 2.0 on the force required to create drop-out at the zero voltage condition. The two shifted regression curves are plotted in Figure 9, one curve for a single, non-magnetic 0.051-mm shim and one for a double, non-magnetic shim or a 0.102 mm total shim thickness. The final margin point for each shim thickness was calculated from the regression curves as the drop-out voltage values corresponding to the maximum possible force from 6 springs plus an additional two times the friction force. An additional 0.1 VDC was added to account for measurement scatter resulting in required minimum drop-out voltage values of 2.05 VDC for the 0.051-mm shim thickness and 3.81 VDC for the 0.102-mm shim thickness. It should be noted that the drop-out voltage of 0.6 measured during acceptance testing of the failed LPA works out to a force factor of safety of 0.97. This was a unit that clearly should have failed.

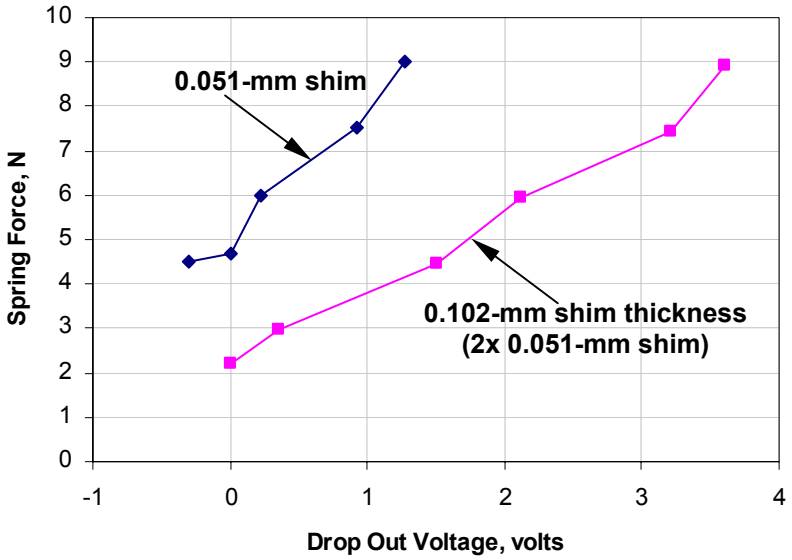

Figure 8. Test data from a spare brake assembly characterizes the variation of drop-out voltage with spring force for two different shim thicknesses.

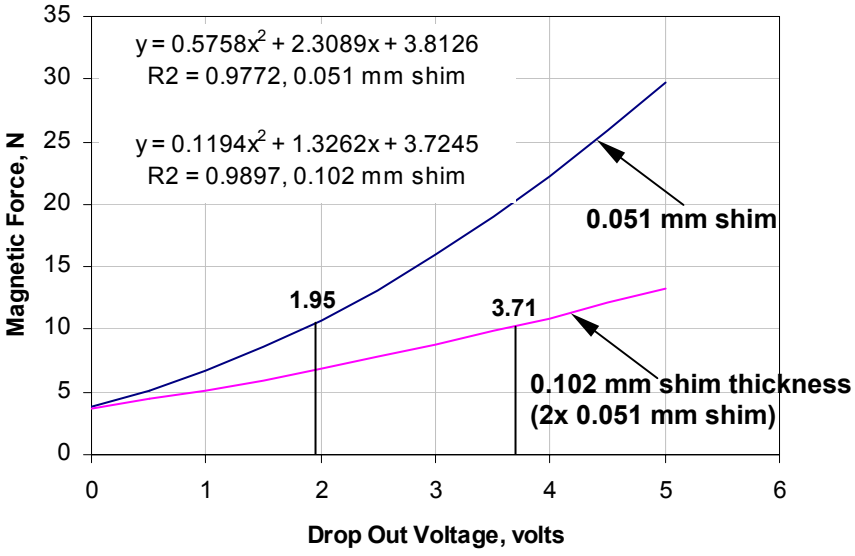

Figure 9. Regression curves from test data are appropriately shifted and used to determine the drop-out voltage required for a minimum 2.0 factor of safety.

Rework

Two flight units, SN 003 and 008, had drop-out voltages of 0.79 VDC and 1.25 VDC respectively, well short of the minimum drop-out voltage of 2.05 VDC required for one shim per the margin analysis. These two units were removed from the second flight lander and transported to Aeroflex Laboratories, Inc. for rework. Rework consisted of adding a second, non-magnetic 0.051-mm shim between the solenoid and the friction plate resulting in a total shim thickness of 0.102 mm. A shim was removed between the brake rotor and the motor rotor to maintain the same brake actuation stroke. The rework was relatively straightforward, however the schedule intensity of the activity was increased substantially due to the proximity of the second launch and the criticality of the LPAs to mission success. The brake housing was carefully removed from the motor housing (Figure 10) after heating the brake housing up at the bond line and removing three screws. Brake housing removal was performed with the brake leads powered so the friction plate was secure against the solenoid. This prevented the friction plate and the compression springs from falling out of the housing during disassembly. The two brake plates are visible in Figure 11a. The brake rotor was removed so that its shimming could be adjusted. The six compression springs are visible after power was removed from the brake assembly to enable removal of the friction plate from the brake housing (Figure 11b). This is the location where the second shim was added after the assembly was cleaned up and inspected. The brake was reassembled. After rework, SN 003 and 008 had drop-out values of 4.09 and 3.85 VDC respectively, which met the minimum requirement of 3.81 VDC for the 0.102 mm shim thickness. Table 4 indicates the performance of these two LPAs, before and after rework.

Dynamics testing was not performed on the reworked LPAs, however, the actuators were exposed to the protoflight temperature range of –120 °C to +60 °C. Each actuator was operated at the voltage extremes of 24 and 32.8 VDC and over the entire output torque range at each acceptance temperature (–60 °C, ambient, +60 °C). There was no change in the torque/speed/current performance or backdrive torque capability from the original acceptance testing. A test to positively confirm brake drop-out after LPA operation in each direction, voltage, and temperature was added. This test consisted of operating the LPA motor with the brake unpowered and verifying that stall current was present. After successfully completing testing, the LPAs were returned to the spacecraft.

The entire process from the initial observation of the failure to the return of the LPAs to the spacecraft took only three weeks and caused no slip in the launch schedule.

Figure 10. The brake assembly is removed from the Lander Petal Actuator during rework to add an additional shim.

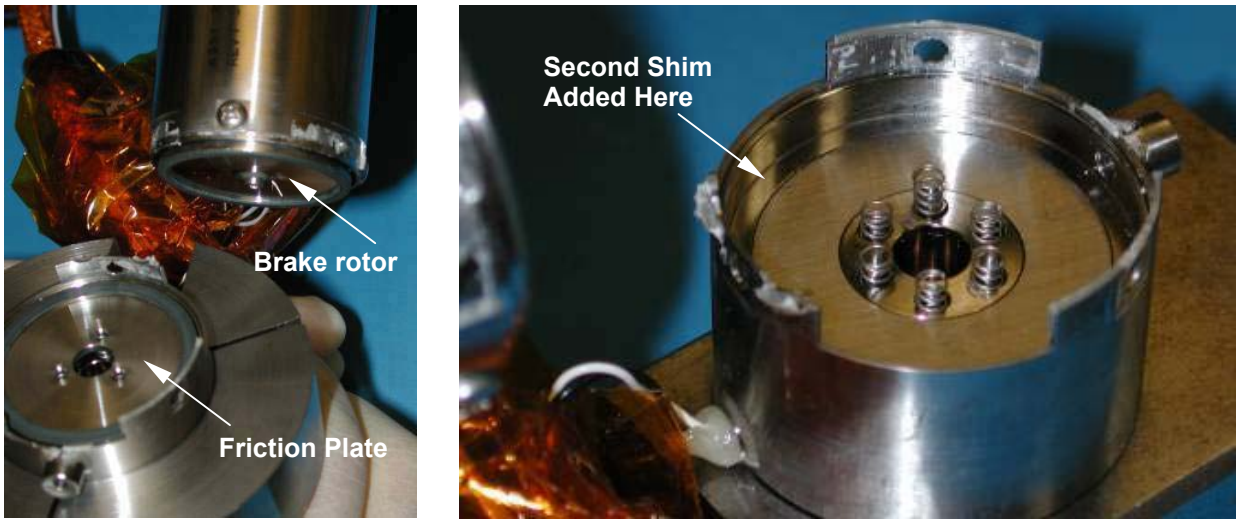

Figure 11a and 11b. Close-up views of the brake assembly during rework

Table 4. Drop-out performance for the reworked brakes

SN	Before Rework (with 0.051-mm shim)		After Rework (with 2x 0.051-mm shim)	
	Drop-Out (VDC)	Force Factor of Safety	Drop-Out (VDC)	Force Factor of Safety
003	0.79	1.08	4.09	2.12
008	1.25	1.38	3.85	2.02

Analysis Using Magnetic Circuit Equations

The results of the failure investigation, the force/drop-out voltage data from the spare brake assembly, and the corresponding margin analysis provided sufficient evidence and understanding to both conclusively attribute the brake failure to residual magnetism and to proceed confidently with the defined rework on two LPAs with marginally acceptable brake assemblies. Some analysis was performed to further explore the source of the unit-to-unit variation in drop-out voltage. The magnetic circuit model of the brake is shown in Figure 12, which leads to the following equation.

$$Ni = (\Phi R)_{CORE} + (\Phi R)_{SHIM} + (\Phi R)_{PLATE} + (\Phi R)_{GAP} \tag{4}$$

where Ni is the value of the magnetomotive force source of the brake coil, N is the number of turns in the coil, i is the current in the coil, Φ is the flux flowing in the magnetic circuit, and R is the reluctance of each component around the circuit. Reluctance of a material with length l along the flux path and cross-sectional area A is defined as

$$R = \frac{l}{\mu A} \tag{5}$$

where μ is the permeability of the material. Higher permeability materials, like the magnetic materials of the brake core and plate, have a lower reluctance and therefore flux flows more easily through them. Since flux is conserved around the magnetic circuit, equation 4 is rewritten as

$$Ni = \Phi\left(R_{CORE} + R_{SHIM} + R_{PLATE} + R_{GAP}\right) \tag{6}$$

The shim is nonmagnetic so its reluctance is that of free space (R_0) just like the air gap. The permeability of both the core and the plate is much higher than the permeability of free space (μ_0), therefore their reluctance is much less than the reluctance of free space resulting in a simplification of equation 6.

$$R_{SHIM} = R_{GAP} = R_0, \;\; R_0 >> R_{CORE}, \;\; R_0 >> R_{PLATE}$$

$$Ni = 2\Phi R_0 = \frac{2\Phi l_0}{\mu_0 A} \tag{7}$$

Making the common assumption that the flux density B is uniform over the cross-sectional area A exposed to the flux results in

$$\Phi = BA \tag{8}$$

The energy stored in the magnetic field in the gap is

$$U = \frac{B^2 l_0 A}{2\mu_0} \tag{9}$$

The magnetic force on the brake plate is equal to the rate of change of energy with the gap length.

$$F_M = \frac{dU}{dl_0} = \frac{B^2 A}{2\mu_0} \tag{10}$$

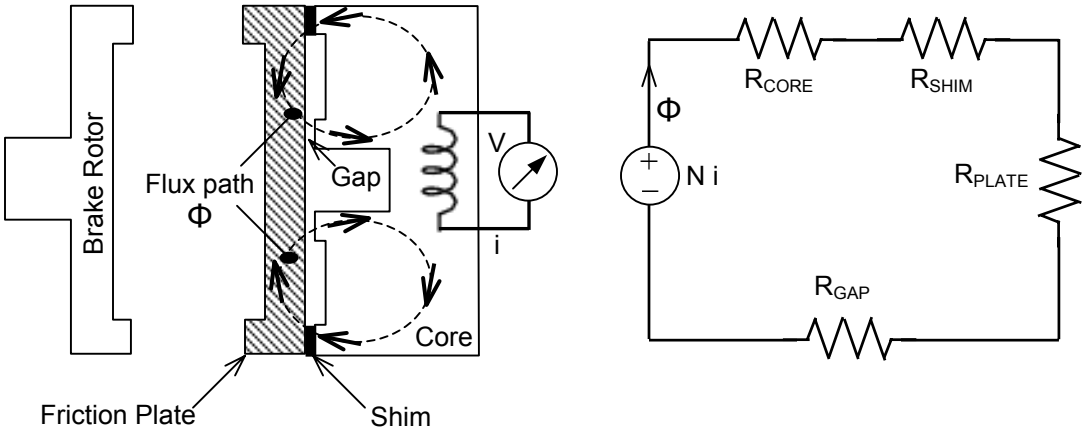

Figure 12. Magnetic circuit model

Substituting equation 8 into equation 7, and combining with equation 10 gives an expression relating the magnetic force on the brake plate to the shim thickness, l_0 .

$$F_M = \frac{N^2 i^2 \mu_0 A}{8 l_0^2} \tag{11}$$

Since force on the friction plate is inversely proportional to the square of the plate's distance from the solenoid, the shim thickness has a large effect on the force balance in the brake assembly. This effect is larger when the friction plate is closer to the solenoid, which is why the addition of a second shim in the brake assembly has a significant effect on the drop-out voltage while having a minor effect on the pull-in voltage. This sensitivity allows the shim modification rework to be effective.

From Ohm's law, current in the solenoid varies with the applied voltage through a constant coil resistance. Using this relationship in equation 11 results in the observation that the drop-out voltage varies linearly with the shim thickness. The shim thickness in the LPAs can vary from 0.0459 mm to 0.0561 mm because of the part tolerances. The expected variation in drop-out voltage from shim thickness variation is a factor of 0.0561/0.0459 = 1.22. This does not account for much of the variation in drop-out voltage seen over the range of LPAs, which is a factor of 6 to 10. At the drop-out position, the unit-to-unit force variation of the 6 springs is 7.65 N to 10.45 N due to the tolerances of the spring parameters and the geometry of the brake assembly. Since drop-out voltage is related to the square root of force, spring force variation could account for a factor of $(10.45/7.65)^{1/2}$ = 1.17, also not sufficient to explain the observed variation.

Equation 6 as written contains the assumption that the only source of magnetomotive force in the solenoid is the brake coil. However the evidence of the residual magnetism in the failed brakes indicates differently. The flux flowing through the solenoid when the brake coil is energized causes the friction plate to magnetize. When power is removed, the friction plate continues to behave as a weak permanent magnet, making it an additional source of magnetomotive force in the solenoid. This behavior is caused by the large hysteresis loop in the B-H curve of the 15-5 PH stainless steel. The core material has a B-H curve with an extremely small hysteresis loop therefore it retains no field. When the additional source of magnetomotive force from the friction plate is added in series with the other elements in the magnet circuit model, equation 6 becomes

$$Ni + mmf_{PLATE} = \Phi\left(R_{CORE} + R_{SHIM} + R_{PLATE} + R_{GAP}\right) \tag{12}$$

Applying the same assumptions as before to equation 12 yields a new version of equation 7.

$$Ni + mmf_{PLATE} = 2\Phi R_0 = \frac{2\Phi l_0}{\mu_0 A} \tag{13}$$

Substituting equation 8 into equation 13, and combining with equation 10 gives a new expression relating the magnetic force on the friction plate to the shim thickness.

$$F_M = \frac{\mu_0 A}{8 l_0^2}\left(mmf_{PLATE} + Ni\right)^2 \tag{14}$$

Table 5 shows the magnetomotive force of the friction plate in the spare brake, which was calculated using equation 14, the data in Table 3, and the geometry of the brake. Table 6 lists the magnetomotive force of the solenoid coil for the typical range of brake drop-out voltage, values which are of the same magnitude as the magnetomotive force of the friction plate. The effect of changes in the magnetomotive force of the friction plate on the drop-out voltage is derived from equation 14. Keeping all other parameters unchanged, decreasing mmf_{PLATE} causes an equivalent increase in Ni. The drop-out voltage increase corresponding to this increase in Ni is determined from $V = \left(Ni\right)\left(R_{COIL}/N\right)$, where R_{COIL} is the coil resistance. A decrease in mmf_{PLATE} of 13.4 causes an increase in drop-out voltage of 1.7 volts since $V = \left(Ni\right)\left(385/3040\right) = \left(Ni\right)\left(0.127\right)$. The exact range of variation of mmf_{PLATE} over all the LPAs is not known but varying this parameter clearly can have a significant effect on the LPA drop-out voltage. The rest of the magnetic circuit and the geometric parameters of the brake are well known, and their variations are insufficient to cause the observed range of drop-out voltage. Therefore, the conclusion is that the majority of the large unit-to-unit variation in drop-out voltage is due to unit-to-unit variation in the magnetic properties of the 15-5 PH stainless steel brake plates. This conclusion is consistent with the experiences of a JPL magnetics expert when dealing with this material.

Table 5. Magnetomotive force of the friction plate in the spare brake

	0.051-mm shim	2x 0.051-mm shim
mmf_{PLATE} (ampere-turns)	13.4	18.4

Table 6. Magnetomotive force of the solenoid coil versus voltage

Voltage (VDC)	1	2	3	4	5
Ni (ampere-turns)	7.9	15.8	23.7	31.6	39.5

Conclusions and Lessons Learned

Given the close tolerances of the parts in the brake assemblies, there was more unit-to-unit difference in drop-out voltage than expected. This was likely due to a larger than expected variation in the magnetic properties of the 15-5 PH stainless steel friction plates, which resulted in a significant differences in the amount of residual magnetism in the magnetic circuit from brake to brake. These variations must be carefully accounted for when using 15-5 PH stainless steel in a magnetic circuit.

Although residual magnetism was recognized as an issue in the design (hence the existence of the non-magnetic 0.051 mm shim), the lack of an appropriately specified lower bound on drop-out voltage prevented brakes with inadequate margin from being discovered and reworked earlier in the flight schedule. More specifically, drop-out should have been treated like any deployment, guaranteeing a minimum force factor of safety of 2.0 that was verified by test.

Acknowledgements

The work described in this paper was performed by the Jet Propulsion Laboratory, California Institute of Technology, under contract with the National Aeronautics and Space Administration.

The effort described in this paper encompassing the discovery of the failure, the failure investigation, the assessment of all LPAs, the rework of two LPAs, and the removal and reinstallation of LPAs on the flight landers, all in a three week period of time, required the combined talents of many people. In particular, the author gratefully acknowledges the contributions of Mike Johnson, Pablo Narvaez, and Don Sevilla of JPL, and Ed Joscelyn and Boz Sharif of Aeroflex Laboratories.

References

1. Gillis-Smith, Greg R. "Mars Pathfinder Lander Deployment Mechanisms." *Proceedings of the 30th Aerospace Mechanism Symposium*, (May 1996), pp. 255-271.
2. Hanselman, Duane. *Brushless Permanent-Magnet Motor Design.* New York: McGraw-Hill, Inc., 1994, pp. 13-59.
3. Wangsness, Roald K. *Electromagnetic Fields.* New York: John Wiley & Sons, 1979, pp. 320-333.
4. Slocum, Alexander H. *Precision Machine Design.* Englewood Cliffs: Prentice Hall, 1992, p. 663.